ISSN: 1672 - 6553

JOURNAL OF DYNAMICS AND CONTROL

VOLUME 9 ISSUE 12: P81-101

# NEWLY GENERATED ORTHOGONAL BESSEL POLYNOMIAL TO SOLVE FINITE BOUNDARY VALUE PROBLEMS, AND INFINITE BOUNDARY VALUE MHD CASSON FLUID FLOWING ACROSS A STRETCHED SHEET

Prithvi S., Patil Mallikarjun B.

Department of Studies and Research in Mathematics, Tumkur University, Jnanasiri Campus, Bidarakatte, Tumakuru, Karnataka - 572 118, India

https://doi.org/10.71058/jodac.v9i12005

# NEWLY GENERATED ORTHOGONAL BESSEL POLYNOMIAL TO SOLVE FINITE BOUNDARY VALUE PROBLEMS, AND INFINITE BOUNDARY VALUE MHD CASSON FLUID FLOWING ACROSS A STRETCHED SHEET

**Prithvi S.[1], Patil Mallikarjun B.[2*]**

*Department of Studies and Research in Mathematics, Tumkur University, Jnanasiri Campus, Bidarakatte, Tumakuru, Karnataka, India - 572 118.*

*[1]prithvirajreddy31@gmail.com, [2]mbp1007@yahoo.com*

***Corresponding Auhor**

**Abstract:** *This article introduces a newly developed Orthogonal Bessel Polynomial and employs the operational matrix of integration approach for solving problems with finite and infinite boundary conditions. In this method, we utilise the Bessel polynomial operational matrix collocation technique to convert the differential equations into a system of nonlinear algebraic equations at various collocating points. These resulting algebraic equations are then solved to obtain the solution to the differential equations. To validate the method, we tested it on multiple problems and observed that the results demonstrated excellent convergence and agreement. For solving differential equations with infinite boundary conditions, we considered the flow of MHD Casson fluid over a permeable stretching sheet, solved the governing equations, and analysed the resulting graphs, providing insights into the behaviour of the system. It could be observed from the calculations below that orthogonal Bessel polynomials provide better results when compared to the non-orthogonal Bessel polynomials.*

**Keywords:** *Bessel Polynomial, Orthogonal, Weight Function, Casson Fluid, Stretching Sheet.*

**Table 1: Nomenclature**

| | | | | |
|---|---|---|---|---|
| $\mu$ | Dynamic viscosity $(kgm^{-1}s^{-1})$ | | $\tau$ | Angle of inclination $(radians)$ |
| $Da^{-1}$ | Inverse darcy number $(-)$ | | $K$ | Permeability constant $(m^2)$ |
| $\nu$ | Kinematic viscosity $(m^2s^{-1})$ | | $\rho$ | Density of the fluid $(kgm^{-3})$ |
| $\sigma$ | Electrical conductivity $(Sm^{-1})$ | | $\beta$ | Casson parameter $(-)$ |

## 1. Introduction

In many diverse domains, polynomials are essential for solving differential equations, providing both numerical and analytical solutions that explain technical and physical phenomena. Modelling real-world systems, from biology and finance to engineering and physics, requires the use of differential equations. These equations may be solved with the use of polynomials, especially orthogonal polynomials, which provide effective computing, approximation, and numerical stability.

https://doi.org/10.71058/jodac.v9i12005

Spectral techniques, which use a sequence of polynomials to estimate functions, are one of the main uses of polynomials in differential equations. Ordinary and partial differential equations are frequently solved using these techniques, which include the Chebyshev and Legendre spectral methods. By expressing the answer as a sum of weighted orthogonal polynomials, spectral techniques provide great precision. Three popular spectrum techniques that make use of polynomial expansions are the collocation[4] and Galerkin[1] approaches. Chebyshev polynomials, in particular, are used in quantum physics, electromagnetics, and computational fluid dynamics because of their capacity to reduce function approximation mistakes.

Polynomials are used in fluid dynamics to solve convection-diffusion equations, magnetohydrodynamics equations, and boundary layer flow issues. Using Chebyshev [2], Matching [24] and Legendre [3] polynomials, the stretching sheet problem, which is a basic subject in boundary layer theory, has been thoroughly investigated. These polynomials are used by researchers to convert the controlling PDEs into a system of nonlinear ODEs, which are then resolved by numerical methods. For instance, the Chebyshev collocation approach [11] effectively manages the flow of both Newtonian and non-Newtonian fluids over sheets that are expanding and contracting. Similarly, polynomial-based spectrum approaches give precise solutions for velocity, temperature, and concentration distributions in magnetohydrodynamics, which studies the interaction of conducting fluids with magnetic fields.

Here we have developed a new orthogonal Bessel polynomials using a weight function. Srivastava [5] presented an overview of the Bessel polynomials, generalised Bessel polynomials, and q-Bessel Polynomials. Frazier and Zhang [6], on the other hand, developed an orthonormal system in which the Bessel wavelet is supported by the Hankel transform, establishing a connection between wavelet theory and integral transforms. Kumbinarasaiah and Preetham [7] analysed the boundary layer flow by Bernoulli wavelets. Ramareddy *et al.* [8] analysed the flow of Casson fluid over a stretching sheet by Fibonacci wavelets. Ramareddy *et al.* [9] analysed the viscoelastic fluid over a stretching sheet by employing the Legendre wavelet. Ramareddy *et al.* [10] examined the unsteady velocity of Williamson fluid flowing over a moving surface using the Hermite wavelet method. They also analysed the streamlines for both 2-D and axisymmetric flow patterns. Suresh *et al.* [11] used the Chebyshev wavelet approach to study the motion of Williamson fluid across a permeable stretched sheet. They discovered that the skin friction coefficient increased as the degree of inclination of the magnetic field increased. In a separate study, Ramareddy *et al.* [12] explored Casson fluid flow over a wedge by applying the Bernoulli wavelet method. They discovered that the fluid velocity increased as the magnetic parameter, Casson parameter, and wedge parameter were raised.

Shiralashetti *et al.* [13] investigated stagnation point flow of Casson fluid across an inclined stretching sheet using the Bernoulli wavelet method. They found that an increase in the Brinkmann number resulted in higher entropy generation. Yadav *et al.* [14] analysed the lumpy skin disease model using Bernstein wavelets and confirmed the efficiency of the Bernstein wavelet method. Finally, Soleyman *et al.* [15] developed the Müntz–Legendre Wavelet Collocation Method for solving the Riccati equation. They performed error analysis and demonstrated the method's

https://doi.org/10.71058/jodac.v9i12005

efficiency and accuracy. Suresh *et al.* [16] applied the Taylor wavelet operational matrix method to analyse Rivlin-Ericksen fluid flow over a stretching sheet. They compared their results with those obtained using the BVP4C method and found excellent agreement between the two approaches. Shiralashetti *et al.* [17] used the Jacobi wavelet method to solve the problem of laminar fluid flow over a porous channel. Their study revealed that the velocity boundary layer thickness decreased as the volume fraction of the nanofluid increased.

Mulimani and Kumbinarasaiah [18] utilised the Gegenbauer wavelet collocation technique to analyse the nonlinear Fisher's equation. They presented several numerical problems to demonstrate the effectiveness and efficiency of the method. Ramareddy *et al.* [19] applied the Fibonacci wavelet frame operational matrix to study Arrhenius-controlled heat transfer over a microchannel. They compared their results with previous studies and found an excellent agreement, further validating the accuracy and reliability of their approach. Dong and Chen [20] employed the Haar wavelet collocation method to analyse fractional pantograph delay differential equations. They validated their results through various numerical experiments, demonstrating both the accuracy and efficiency of the proposed method. Raza *et al.* [21] used the Hermite wavelet collocation technique to solve 3-D partial differential equations. To assess the accuracy of their approach, they solved the Helmholtz and Poisson equations and found excellent agreement with the expected results, confirming the high precision of the method. Using a three-dimensional model, Nadeem *et al.* [22] investigated the flow of Casson fluid over a linearly expanding sheet. They found that the skin friction coefficients increased with higher values of the Hartmann number and porousness parameter. Ahmad *et al.* [23] analysed Casson fluid flow across a stretching sheet to examine heat transfer

In the present study, we have developed an orthogonal Bessel polynomial based on the Bessel polynomial using the Gram-Schmidt orthogonalisation technique. From this, we generated an operational matrix of integration using these polynomials. This generated matrix was then applied to solve nonlinear differential equations with finite boundary conditions. Additionally, we extended our approach to solve a differential equation with infinite boundary conditions, modelling the flow of MHD Casson fluid over a stretching sheet. The results obtained were compared with both exact and analytical solutions, showing a remarkable agreement, further validating the effectiveness of our method. It could be observed from our study that orthogonal Bessel polynomials provided better results in comparison with the non-orthogonal Bessel polynomials.

## 2. Orthogonal Bessel Polynomial

The Bessel polynomial is obtained by solving the following differential equation [5]:

$$\frac{d^2y(x)}{dx^2} + 2(x+2)\frac{dy(x)}{dx} - n(n+1)y(x) = 0 \tag{1}$$

The Bessel polynomial satisfies the following recurrence realtion:

$$y_{n+1}(x) = (2n+1)xy_n(x) + y_{n-1}(x) \tag{2}$$

where $y_0 = 1$ and $y_1 = 1 + x$

Which yields the following sequence of polynomials:

https://doi.org/10.71058/jodac.v9i12005

$y_2 = 3x^2 + 3x + 1$
$y_3 = 15x^3 + 15x^2 + 6x + 1$
$y_4 = 105x^4 + 105x^3 + 45x^2 + 10x + 1$
$y_5 = 945x^5 + 945x^4 + 420x^3 + 105x^2 + 15x + 1$ .
.
.
.
$$y_{10} = 654729075x^{10} + 654729075x^9 + 310134825x^8 + 91891800x^7 + 18918900x^6 + 2837835x^5 + 315315x^4 + 25740x^3 + 1485x^2 + 55x + 1$$

These polynomials are not orthogonal. We orthogonalize the polynomials wrt weight function 1 and wrt weight function $\frac{1}{\sqrt{1-x^2}}$ and get 2 sets of orthogonal polynomials.

The orthogonal polynomials concerning the weight function 1 are as follows:

$r_0 = 1$
$r_1 = x$
$$r_2 = 3x^2 - \frac{3}{2}$$
$$r_3 = \frac{15x(4x^2-3)}{4}$$
$$r_4 = 105x^4 - 105x^2 + \frac{105}{8}$$
$$r_5 = \frac{945x(16x^4 - 20x^2 + 5)}{16}$$
$$r_6 = 10395x^6 - \frac{31185x^4}{2} + \frac{93555x^2}{16} - \frac{10395}{32}$$
$$r_7 = \frac{135135x(64x^6 - 112x^4 + 56x^2 - 7)}{64}$$
$$r_8 = 2027025x^8 - 4054050x^6 + \frac{10135125 * x^4}{4} - \frac{2027025x^2}{4} + \frac{2027025}{128}$$
$$r_9 = \frac{34459425x(256x^8 - 576x^6 + 432x^4 - 120x^2 + 9)}{256}$$

The orthogonal polynomials with respect to the weight function $\frac{1}{\sqrt{1-x^2}}$ are as follows:

$t_0 = 1$
$t_1 = x$
$$t_2 = 3x^2 - \frac{3}{2}$$
$$t_3 = \frac{15x(4x^2-3)}{4}$$

https://doi.org/10.71058/jodac.v9i12005

$$t_4 = 105x^4 - 105x^2 + \frac{105}{8}$$
$$t_5 = \frac{945x(16x^4 - 20x^2 + 5)}{16}$$
$$t_6 = 10395x^6 - \frac{31185x^4}{2} + \frac{93555 * x^2}{16} - \frac{10395}{32}$$
$$t_7 = \frac{135135x(64x^6 - 112x^4 + 56x^2 - 7)}{64}$$
$$t_8 = 2027025x^8 - 4054050x^6 + \frac{10135125x^4}{4} - \frac{2027025x^2}{4} + \frac{2027025}{128}$$
$$t_9 = \frac{34459425x(256x^8 - 576x^6 + 432x^4 - 120x^2 + 9)}{256}$$
$$t_{10} = 654729075x^{10} - \frac{3273645375x^8}{2} + \frac{22915517625x^6}{16} - \frac{16368226875x^4}{32} + \frac{16368226875x^2}{256} - \frac{654729075}{512}$$

### 2.1 Function Approximation:

$F(x)$ expressed by means of the Bessel Polynomials:

$$F(x) = \sum_{m=0}^{\infty} Z_m \chi_m(x). \tag{3}$$

Where $\chi_i(x),\ i = 0,1,2,\dots\infty$ are orthogonalized or non-orthogonalized bessel polynomials.
Truncating the series we get finite number of terms as:

$$F(x) \approx \sum_{m=0}^{M-1} Z_m \chi_m(x) = Z^T B_w(x). \tag{4}$$

where $Z^T$ is $1 \times M$ matrix and $B_w(x)$ is $M \times 1$ matrix, $Z^T = [Z_0, Z_1 Z_2 \dots\dots Z_{M-1}]$ and $(B_w(x))^T = [\chi_0, \chi_1, \chi_2 \dots \chi_{M-1}]$

Where $Z^T$ is the unknown coefficient matrix to be obtained. $B_w(x)$ are the orthogonalized or non-orthogonalized Bessel polynomials. Here we consider $10$ such polynomials and hence $M = 10$. Therfore let $B_{y10}(x) = [y_0 \quad y_1 \quad y_2 \quad y_3 \quad y_4 \quad y_5 \quad y_6 \quad y_7 \quad y_8 \quad y_9]^T$, $B_{r10}(x) = [r_0 \quad r_1 \quad r_2 \quad r_3 \quad r_4 \quad r_5 \quad r_6 \quad r_7 \quad r_8 \quad r_9]^T$ , $B_{t10}(x) = [t_0 \quad t_1 \quad t_2 \quad t_3 \quad t_4 \quad t_5 \quad t_6 \quad t_7 \quad t_8 \quad t_9]^T$

## 3. Operational matrix of Integration

### 3.1 Operational matrix of Integration for Bessel Polynomials :

Integrate $y_m(x)$ wrt $x$ and expressing as a linear combination of Bessel polynomials.
$\int_0^x y_0(x)dx = [-1 \quad 1 \quad 0 \quad 0 \quad 0 \quad 0 \quad 0 \quad 0 \quad 0 \quad 0]B_{y10}(x),$
$\int_0^x y_1(x)dx = [\frac{-2}{3} \quad \frac{1}{2} \quad \frac{1}{6} \quad 0 \quad 0 \quad 0 \quad 0 \quad 0 \quad 0 \quad 0]B_{y10}(x),$

https://doi.org/10.71058/jodac.v9i12005

$$\int_0^x y_2(x)dx = [\tfrac{-1}{3} \quad \tfrac{1}{10} \quad \tfrac{1}{6} \quad \tfrac{1}{15} \quad 0 \quad 0 \quad 0 \quad 0 \quad 0 \quad 0]B_{y10}(x),$$
$$\int_0^x y_3(x)dx = [\tfrac{-1}{6} \quad 0 \quad \tfrac{1}{21} \quad \tfrac{1}{12} \quad \tfrac{1}{28} \quad 0 \quad 0 \quad 0 \quad 0 \quad 0]B_{y10}(x),$$
$$\int_0^x y_4(x)dx = [\tfrac{-1}{10} \quad 0 \quad 0 \quad \tfrac{1}{36} \quad \tfrac{1}{20} \quad \tfrac{1}{45} \quad 0 \quad 0 \quad 0 \quad 0]B_{y10}(x),$$
$$\int_0^x y_5(x)dx = [\tfrac{-1}{15} \quad 0 \quad 0 \quad 0 \quad \tfrac{1}{55} \quad \tfrac{1}{30} \quad \tfrac{1}{66} \quad 0 \quad 0 \quad 0]B_{y10}(x),$$
$$\int_0^x y_6(x)dx = [\tfrac{-12586}{264305} \quad 0 \quad 0 \quad 0 \quad 0 \quad \tfrac{7161}{558559} \quad \tfrac{1}{42} \quad \tfrac{1}{91} \quad 0 \quad 0]B_{y10}(x),$$
$$\int_0^x y_7(x)dx = [\tfrac{-552}{15455} \quad \tfrac{2}{381539} \quad \tfrac{-3}{779972} \quad 0 \quad 0 \quad 0 \quad \tfrac{1}{105} \quad \tfrac{1}{56} \quad \tfrac{1}{120} \quad 0]B_{y10}(x),$$
$$\int_0^x y_8(x)dx = [\tfrac{-98}{3527} \quad \tfrac{5}{291178} \quad \tfrac{-6}{527903} \quad 0 \quad \tfrac{2}{535539} \quad 0 \quad 0 \quad \tfrac{1712}{232831} \quad \tfrac{1}{72} \quad \tfrac{1}{153}]B_{y10}(x),$$
$$\int_0^x y_9(x)dx = \left[\tfrac{-227}{10014} \quad \tfrac{47}{48966} \quad \tfrac{-35}{57437} \quad \tfrac{-2}{30043} \quad \tfrac{19}{93926} \quad \tfrac{-9}{184414} \quad \tfrac{-2}{605191} \quad \tfrac{1}{636630} \quad \tfrac{965}{165016} \quad \tfrac{11070}{996301}\right] B_{y10}(x) + \tfrac{1}{190} y_{11}(x),$$

This implies,

$$\int_0^x B_{y10}(x)dx = S_{10\times10}B_{y10}(x) + \hat{B}_{y10}(x),$$

where

$$S = \begin{bmatrix} -1 & 1 & 0 & 0 & 0 & 0 & 0 & 0 & 0 & 0 \\ \frac{-2}{3} & \frac{1}{2} & \frac{1}{6} & 0 & 0 & 0 & 0 & 0 & 0 & 0 \\ \frac{-1}{3} & \frac{1}{10} & \frac{1}{6} & \frac{1}{15} & 0 & 0 & 0 & 0 & 0 & 0 \\ \frac{-1}{6} & 0 & \frac{1}{21} & \frac{1}{12} & \frac{1}{28} & 0 & 0 & 0 & 0 & 0 \\ \frac{-1}{10} & 0 & 0 & \frac{1}{36} & \frac{1}{20} & \frac{1}{45} & 0 & 0 & 0 & 0 \\ \frac{-1}{15} & 0 & 0 & 0 & \frac{1}{55} & \frac{1}{30} & \frac{1}{66} & 0 & 0 & 0 \\ \frac{-12586}{264305} & 0 & 0 & 0 & 0 & \frac{7161}{558559} & \frac{1}{42} & \frac{1}{91} & 0 & 0 \\ \frac{-552}{15455} & \frac{2}{381539} & \frac{-3}{779972} & 0 & 0 & 0 & \frac{1}{105} & \frac{1}{56} & \frac{1}{120} & 0 \\ \frac{-98}{3527} & \frac{5}{291178} & \frac{-6}{527903} & 0 & \frac{2}{535539} & 0 & 0 & \frac{1712}{232831} & \frac{1}{72} & \frac{1}{153} \\ \frac{-227}{10014} & \frac{47}{48966} & \frac{-35}{57437} & \frac{-2}{30043} & \frac{19}{93926} & \frac{-9}{184414} & \frac{-2}{605191} & \frac{1}{636630} & \frac{965}{165016} & \frac{11070}{996301} \end{bmatrix}$$

https://doi.org/10.71058/jodac.v9i12005

$$\hat{B}_{y10}(x) = \begin{bmatrix} 0 \\ 0 \\ 0 \\ 0 \\ 0 \\ 0 \\ 0 \\ 0 \\ 0 \\ \frac{1}{190} y_{11}(x) \end{bmatrix}$$

Integrating $B_{y10}(x)$ twice we get

$$\int_0^x \int_0^x B_{y10}(x)dxdx = S'_{10\times10} B_{y10}(x) + \hat{B}'_{y10}(x),$$

and thrice we get

$$\int_0^x \int_0^x \int_0^x B_{y10}(x)dxdxdx = S''_{10\times10} B_{y10}(x) + \hat{B}''_{y10}(x),$$

In the similar way we can obtain higher order operational matrix of integration

## 3.2 Operational matrix of Integration for Orthogoanl Bessel Polynomials wrt Weight function 1 :

Integrate $r_m(x)$ wrt $x$ and expressing as a linear combination of Bessel polynomials.

$\int_0^x r_0(x)dx = [0 \quad 1 \quad 0 \quad 0 \quad 0 \quad 0 \quad 0 \quad 0 \quad 0 \quad 0]B_{r10}(x),$

$\int_0^x r_1(x)dx = [\frac{1}{6} \quad 0 \quad \frac{1}{6} \quad 0 \quad 0 \quad 0 \quad 0 \quad 0 \quad 0 \quad 0]B_{r10}(x),$

$\int_0^x r_2(x)dx = [0 \quad \frac{-2}{5} \quad 0 \quad \frac{1}{15} \quad 0 \quad 0 \quad 0 \quad 0 \quad 0 \quad 0]B_{r10}(x),$

$\int_0^x r_3(x)dx = [\frac{-3}{4} \quad 0 \quad \frac{-3}{7} \quad 0 \quad \frac{1}{28} \quad 0 \quad 0 \quad 0 \quad 0 \quad 0]B_{r10}(x),$

$\int_0^x r_4(x)dx = [0 \quad 0 \quad 0 \quad \frac{-4}{9} \quad 0 \quad \frac{1}{45} \quad 0 \quad 0 \quad 0 \quad 0]B_{r10}(x),$

$\int_0^x r_5(x)dx = [\frac{15}{2} \quad 0 \quad 0 \quad 0 \quad \frac{-5}{11} \quad 0 \quad \frac{1}{66} \quad 0 \quad 0 \quad 0]B_{r10}(x),$

$\int_0^x r_6(x)dx = [0 \quad 0 \quad 0 \quad 0 \quad 0 \quad \frac{-6}{13} \quad 0 \quad \frac{1}{91} \quad 0 \quad 0]B_{r10}(x),$

$\int_0^x r_7(x)dx = [\frac{-1575}{8} \quad 0 \quad 0 \quad 0 \quad 0 \quad 0 \quad \frac{-7}{15} \quad 0 \quad \frac{1}{120} \quad 0]B_{r10}(x),$

$\int_0^x r_8(x)dx = [0 \quad 0 \quad 0 \quad 0 \quad 0 \quad 0 \quad 0 \quad \frac{-8}{17} \quad 0 \quad \frac{1}{153}]B_{r10}(x),$

$\int_0^x r_9(x)dx = [\frac{19845}{2} \quad 0 \quad 0 \quad 0 \quad 0 \quad 0 \quad 0 \quad 0 \quad \frac{-9}{19} \quad 0]B_{r10}(x) + \frac{1}{190} r_{11}(x),$

This implies,

$$\int_0^x B_{r10}(x)dx = W_{10\times10} B_{r10}(x) + \hat{B}_{r10}(x),$$

where

https://doi.org/10.71058/jodac.v9i12005

$$W = \begin{bmatrix} 0 & 1 & 0 & 0 & 0 & 0 & 0 & 0 & 0 & 0 \\ \frac{1}{6} & 0 & \frac{1}{6} & 0 & 0 & 0 & 0 & 0 & 0 & 0 \\ 0 & \frac{-2}{5} & 0 & \frac{1}{15} & 0 & 0 & 0 & 0 & 0 & 0 \\ \frac{-3}{4} & 0 & \frac{-3}{7} & 0 & \frac{1}{28} & 0 & 0 & 0 & 0 & 0 \\ 0 & 0 & 0 & \frac{-4}{9} & 0 & \frac{1}{45} & 0 & 0 & 0 & 0 \\ \frac{15}{2} & 0 & 0 & 0 & \frac{-5}{11} & 0 & \frac{1}{66} & 0 & 0 & 0 \\ 0 & 0 & 0 & 0 & 0 & \frac{-6}{13} & 0 & \frac{1}{91} & 0 & 0 \\ \frac{-1575}{8} & 0 & 0 & 0 & 0 & 0 & \frac{-7}{15} & 0 & \frac{1}{120} & 0 \\ 0 & 0 & 0 & 0 & 0 & 0 & 0 & \frac{-8}{17} & 0 & \frac{1}{153} \\ \frac{19845}{2} & 0 & 0 & 0 & 0 & 0 & 0 & 0 & \frac{-9}{19} & 0 \end{bmatrix} \text{ and } \hat{B}_{r10}(x) = \begin{bmatrix} 0 \\ 0 \\ 0 \\ 0 \\ 0 \\ 0 \\ 0 \\ 0 \\ 0 \\ \frac{1}{190} r_{11}(x) \end{bmatrix},$$

Integrating $B_{r10}(x)$ twice we get

$$\int_0^x \int_0^x B_{r10}(x)dxdx = W'_{10\times10} B_{r10}(x) + \widehat{B}'_{r10}(x),$$

and thrice we get

$$\int_0^x \int_0^x \int_0^x B_{r10}(x)dxdxdx = W''_{10\times10} B_{r10}(x) + \widehat{B}''_{r10}(x),$$

Similarly, we can obtain a higher-order operational matrix of integration

## 3.3 Operational matrix of Integration for Orthogonal Bessel Polynomials wrt Weight function $\frac{1}{\sqrt{1-x^2}}$ :

Integrate $t_m(x)$ wrt $x$ and expressed as a linear combination of Bessel polynomials.

$\int_0^x t_0(x)dx = [0 \quad 1 \quad 0 \quad 0 \quad 0 \quad 0 \quad 0 \quad 0 \quad 0 \quad 0] B_{t10}(x),$

$\int_0^x t_1(x)dx = [\frac{1}{4} \quad 0 \quad \frac{1}{6} \quad 0 \quad 0 \quad 0 \quad 0 \quad 0 \quad 0 \quad 0] B_{t10}(x),$

$\int_0^x t_2(x)dx = [0 \quad \frac{-3}{4} \quad 0 \quad \frac{1}{15} \quad 0 \quad 0 \quad 0 \quad 0 \quad 0 \quad 0] B_{t10}(x),$

$\int_0^x t_3(x)dx = [\frac{-45}{32} \quad 0 \quad \frac{-5}{8} \quad 0 \quad \frac{1}{28} \quad 0 \quad 0 \quad 0 \quad 0 \quad 0] B_{t10}(x),$

$\int_0^x t_4(x)dx = [0 \quad 0 \quad 0 \quad \frac{-7}{12} \quad 0 \quad \frac{1}{45} \quad 0 \quad 0 \quad 0 \quad 0] B_{t10}(x),$

$\int_0^x t_5(x)dx = [\frac{1575}{128} \quad 0 \quad 0 \quad 0 \quad \frac{-9}{16} \quad 0 \quad \frac{1}{66} \quad 0 \quad 0 \quad 0] B_{t10}(x),$

$\int_0^x t_6(x)dx = [0 \quad 0 \quad 0 \quad 0 \quad 0 \quad \frac{-11}{20} \quad 0 \quad \frac{1}{91} \quad 0 \quad 0] B_{t10}(x),$

$\int_0^x t_7(x)dx = [\frac{-12317}{40} \quad 0 \quad 0 \quad 0 \quad 0 \quad 0 \quad 0 \quad \frac{-13}{24} \quad 0 \quad \frac{1}{120}] B_{t10}(x),$

$\int_0^x t_8(x)dx = [0 \quad 0 \quad 0 \quad 0 \quad 0 \quad 0 \quad 0 \quad \frac{-15}{28} \quad 0 \quad \frac{1}{153}] B_{t10}(x),$

https://doi.org/10.71058/jodac.v9i12005

$\int_0^x t_9(x)dx = [\frac{151433}{10} \quad 0 \quad 0 \quad 0 \quad 0 \quad 0 \quad 0 \quad 0 \quad \frac{-17}{32} \quad 0]B_{t10}(x) + \frac{1}{190}t_{11}(x),$

This implies,

$$\int_0^x B_{t10}(x)dx = Q_{10\times10}B_{t10}(x) + \hat{B}_{t10}(x),$$

Where

$$Q = \begin{bmatrix} 0 & 1 & 0 & 0 & 0 & 0 & 0 & 0 & 0 & 0 \\ \frac{1}{4} & 0 & \frac{1}{6} & 0 & 0 & 0 & 0 & 0 & 0 & 0 \\ 0 & \frac{-3}{4} & 0 & \frac{1}{15} & 0 & 0 & 0 & 0 & 0 & 0 \\ \frac{-45}{32} & 0 & \frac{-5}{8} & 0 & \frac{1}{28} & 0 & 0 & 0 & 0 & 0 \\ 0 & 0 & 0 & \frac{-7}{12} & 0 & \frac{1}{45} & 0 & 0 & 0 & 0 \\ \frac{1575}{128} & 0 & 0 & 0 & \frac{-9}{16} & 0 & \frac{1}{66} & 0 & 0 & 0 \\ 0 & 0 & 0 & 0 & 0 & \frac{-11}{20} & 0 & \frac{1}{91} & 0 & 0 \\ \frac{-12317}{40} & 0 & 0 & 0 & 0 & 0 & 0 & \frac{-13}{24} & 0 & \frac{1}{120} \\ 0 & 0 & 0 & 0 & 0 & 0 & 0 & \frac{-15}{28} & 0 & \frac{1}{153} \\ \frac{151433}{10} & 0 & 0 & 0 & 0 & 0 & 0 & 0 & \frac{-17}{32} & 0 \end{bmatrix} \text{ and } \hat{B}_{t10}(x) = \begin{bmatrix} 0 \\ 0 \\ 0 \\ 0 \\ 0 \\ 0 \\ 0 \\ 0 \\ 0 \\ \frac{1}{190}t_{11}(x) \end{bmatrix}$$

Integrating $B_{t10}(x)$ twice we get

$$\int_0^x \int_0^x B_{t10}(x)dxdx = Q'_{10\times10}B_{t10}(x) + \widehat{B}'_{t10}(x),$$

and thrice we get

$$\int_0^x \int_0^x \int_0^x B_{t10}(x)dxdxdx = Q''_{10\times10}B_{t10}(x) + \widehat{B}''_{t10}(x),$$

Similarly, we can obtain a higher-order operational matrix of integration

## 4. Numerical Experiments

**Problem 1:** Let's consider the following differential equation [4]

$$y''(x) + (y'(x))^2 - y(x) = sinh^2(x), 0 < x < 1 \qquad (1)$$

with boundary conditions

$$y(0) = 1, y(1) = cosh(1) \qquad (2)$$

This equation has an exact solution $y(x) = cosh(x)$

**Numerical Implementation:**

Assume

$$y''(x) = Z_1^T B_{y10(x)} \qquad (3)$$

where $Z_1^T = [\ a_1, \ a_2, \ a_3, \ a_4, \ a_5, \ a_6, \ a_7, \ a_8, \ a_9, \ a_{10}\ ]$ is an unknown coefficient matrix

On integrating Eq.(10) wrt x from 0 to x, we get

$$y'(x) = y'(0) + Z_1^T(S_{10\times10}B_{y10}(x) + \hat{B}_{y10}(x)) \qquad (4)$$

Again, integrating Eq.(11) wrt x from 0 to x, we get

https://doi.org/10.71058/jodac.v9i12005

$$y(x) = 1 + xy'(0) + Z_1^T(S'_{10\times10}B_{y10}(x) + \hat{B}_{y10}{}'(x)) \quad (5)$$

we have $y(1) = cosh(1)$, thus on substituting this in Eq.(12) we get

$$y'(0) = cosh(1) - 1 - Z_1^T(S'_{10\times10}B_{y10}(x) + \hat{B}_{y10}{}'(x)) \quad (6)$$

Now substituting Eq.(7) into Eq.(10) in Eq.(8) and collocating this equation with collocating points $x_i = \frac{2i-1}{20}$ $for$ $i = 1,2,3,4,5,6,7,8,9,10$, we obtain a system of nonlinear simultaneous equations with unknown coefficients. On solving these unknown coefficients by MATLAB, we get the unknown coefficients, which, on substituting in Eq.(7) to Eq.(10) we obtain $y(x), y''(x)$ and $y''(x)$.

The unknown coefficients $Z_1^T$ is

$$Z_1^T = [\ \frac{1592}{2589}\ \ \frac{1199}{2368}\ \ \frac{823}{3009}\ \ \frac{-641}{10609}\ \ \frac{-452}{1665}\ \ \frac{217}{1817}\ \ \frac{-306}{19139}\ \ \frac{16}{23125}\ \ \frac{1}{850914}\ \ 0\ ]$$

On resubstituting this $Z_1^T$ into Eq.(7) to Eq.(10) we get $y'(0),\quad y(x),\quad y'(x),\quad y''(x)$

$$y(x) = -0.127405089x^{11} - 0.1292487382x^{10} + 1.240083019x^9 - 1.312702623x^8 - 0.244119589x^7 + 0.693434427x^6 + 0.1392748232x^5 - 0.2381462123x^4 - 0.04588456035x^3 + 0.5834983007x^2 - 0.01570312086x + 0.9999999979 \quad (8)$$

The numerical implementation is similar for orthogonal polynomials as well.

Thus, for orthogonal Bessel polynomials wrt the weight function 1, we get unknown coefficients $Z_2^T$ as

$$Z_2^T = [\ \frac{1089}{1192}\ \ \frac{1126}{2387}\ \ \frac{768}{4987}\ \ \frac{-281}{2323}\ \ \frac{599}{11081}\ \ \frac{-46}{4213}\ \ \frac{47}{36924}\ \ \frac{-26}{291529}\ \ \frac{3}{835966}\ \ 0\ ]$$

On resubstituting this $Z_2^T$ into Eq.(7) to Eq.(10) we get $y'(0),\quad y(x),\quad y'(x),\quad y''(x)$

$$y(x) = 0.4996321408x^2 - 0.0003231586225x(429x^6 - 693x^4 + 315x^2 - 35) - 0.0000002399892916x(88179x^10 - 230945x^8 + 218790x^6 - 90090x^4 + 15015x^2 - 693) - 0.00001269831277x(12155x^8 - 25740x^6 + 18018x^4 - 4620x^2 + 315) - 0.02353870164x + 0.1261765747x^3 + 0.01557973079x^4 - 0.151111263x^6 - 0.006197730706x^8 + 0.08082565109x^{10} + 0.001071448998x(63x^4 - 70x^2 + 15) + 1.0 \quad (9)$$

For orthogonal Bessel polynomials wrt the weight function $\frac{1}{\sqrt{1-x^2}}$ we get unknown coefficients $Z_3^T$ as

$$Z_3^T = [\ \frac{1089}{1192}\ \ \frac{1126}{2387}\ \ \frac{768}{4987}\ \ \frac{-281}{2323}\ \ \frac{599}{11081}\ \ \frac{-46}{4213}\ \ \frac{47}{36924}\ \ \frac{-26}{291529}\ \ \frac{3}{835966}\ \ 0\ ]$$

On resubstituting this $Z_3^T$ into Eq.(7) to Eq.(10) we get $y'(0),\quad y(x),\quad y'(x),\quad y''(x)$

$$y(x) = 0.0000002234300236x + 0.0000001404620569x(4x^2 - 3) + 2.645389695 \times 10^{-11}x(1024x^{10} - 2816x^8 + 2816x^6 - 1232x^4 + 220x^2 - 11) + 0.00000001134914273x(64x^6 - 112x^4 + 56x^2 - 7) + 0.00000005357136389x(16x^4 - 20x^2 + 5) + 0.000000001092919549x(256x^8 - 576x^6 + 432x^4 - 120x^2 + 9) + 0.5x^2 + 0.04166666146x^4 + 0.001388807364x^6 + 0.00002456599299x^8 + 0.0000001701038084x^{10} + 1 \quad (10)$$

https://doi.org/10.71058/jodac.v9i12005

**Table 2: Comparison of $y(x)$ with exact solution for problem 1 by non-orthogonal Bessel polynomials [4]**

| $x$ | exact solution [4] | Present Method | Absolute Error |
|---|---|---|---|
| 0 | 1 | 0.999999997850454 | $2.149545652585516\times 10^{-09}$ |
| 0.1 | 1.005004168055804 | 1.004197019459414 | $8.071485963894176\times 10^{-04}$ |
| 0.2 | 1.020066755619076 | 1.019534276858869 | $5.324787602067893\times 10^{-04}$ |
| 0.3 | 1.045338514128860 | 1.045363897007994 | $2.538287913367299\times 10^{-05}$ |
| 0.4 | 1.081072371838455 | 1.081357729848286 | $2.853580098314268\times 10^{-04}$ |
| 0.5 | 1.127625965206381 | 1.127789234672908 | $1.632694665270051\times 10^{-04}$ |
| 0.6 | 1.185465218242268 | 1.185416876962027 | $4.834128024056028\times 10^{-05}$ |
| 0.7 | 1.255169005630943 | 1.255087116377476 | $8.188925346686027\times 10^{-05}$ |
| 0.8 | 1.337434946304845 | 1.337444669616795 | $9.723311950482483\times 10^{-06}$ |
| 0.9 | 1.433086385448775 | 1.433112289776802 | $2.590432802707099\times 10^{-05}$ |

**Table 3: Comparison of $y(x)$ with exact solution for problem 1 by orthogonal Bessel polynomials wrt weight function 1 [4]**

| $x$ | exact solution [4] | Present Method | Absolute Error |
|---|---|---|---|
| 0 | 1 | 0.999999999988787 | $1.121303050410916\times 10^{-11}$ |
| 0.1 | 1.005004168055804 | 1.005004020275429 | $1.477803743821227\times 10^{-07}$ |
| 0.2 | 1.020066755619076 | 1.020066717161464 | $3.845761153975502\times 10^{-08}$ |
| 0.3 | 1.045338514128860 | 1.045338415470315 | $9.865854577739697\times 10^{-08}$ |
| 0.4 | 1.081072371838455 | 1.081072248502612 | $1.233358426500075\times 10^{-07}$ |
| 0.5 | 1.127625965206381 | 1.127625937973022 | $2.723335867926835\times 10^{-08}$ |
| 0.6 | 1.185465218242268 | 1.185465132129988 | $8.611227997334936\times 10^{-08}$ |
| 0.7 | 1.255169005630943 | 1.255168895139315 | $1.104916280691981\times 10^{-07}$ |
| 0.8 | 1.337434946304845 | 1.337434902573261 | $4.373158346560047\times 10^{-08}$ |
| 0.9 | 1.433086385448775 | 1.433086251659773 | $1.337890012109710\times 10^{-07}$ |

**Table 4: Comparison of $y(x)$ with exact solution for problem 1 by orthogonal Bessel polynomials wrt weight function $\frac{1}{\sqrt{1-x^2}}$ [4]**

| $x$ | exact solution [4] | Present Method | Absolute Error |
|---|---|---|---|
| 0 | 1 | 0.999999999998787 | $1.212585587495596\times 10^{-12}$ |
| 0.1 | 1.005004168055804 | 1.005004168054692 | $1.111555292254707\times 10^{-12}$ |
| 0.2 | 1.020066755619076 | 1.020066755618101 | $9.752199048307375\times 10^{-13}$ |
| 0.3 | 1.045338514128860 | 1.045338514128007 | $8.537615059367454\times 10^{-13}$ |

https://doi.org/10.71058/jodac.v9i12005

| | | | |
|---|---|---|---|
| 0.4 | 1.081072371838455 | 1.081072371837699 | $7.560618797697316\times 10^{-13}$ |
| 0.5 | 1.127625965206381 | 1.127625965205749 | $6.312728118018640\times 10^{-13}$ |
| 0.6 | 1.185465218242268 | 1.185465218241817 | $4.507505479978136\times 10^{-13}$ |
| 0.7 | 1.255169005630943 | 1.255169005630620 | $3.226308109560705\times 10^{-13}$ |
| 0.8 | 1.337434946304845 | 1.337434946304594 | $2.502442697505103\times 10^{-13}$ |
| 0.9 | 1.433086385448775 | 1.433086385448678 | $9.681144774731365\times 10^{-14}$ |

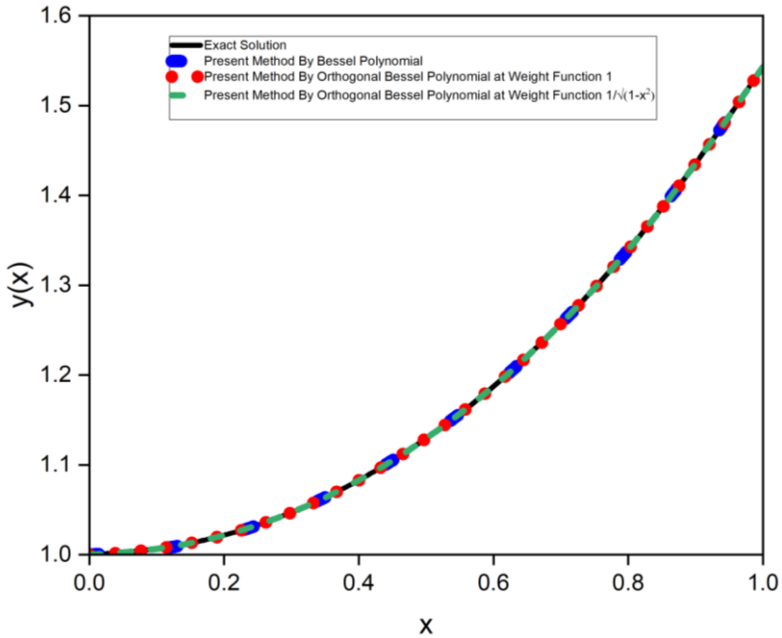


**Figure 1:** Exact versus Present method for Problem 1

**Problem 2: Analysis of the MHD Casson fluid flowing over a permeable stretching sheet**

In this case, we consider a laminar Casson fluid boundary layer flow across a permeable stretched sheet with the magnetic field oriented at $\tau$. Using the assumption that the y-coordinate is orthogonal to the flow and that the x-coordinate is taken horizontally across the surface. The ambient velocity is $U_w = sx$, where $s$ is the stretching constant. The above consideration is shown in Figure 3.

https://doi.org/10.71058/jodac.v9i12005

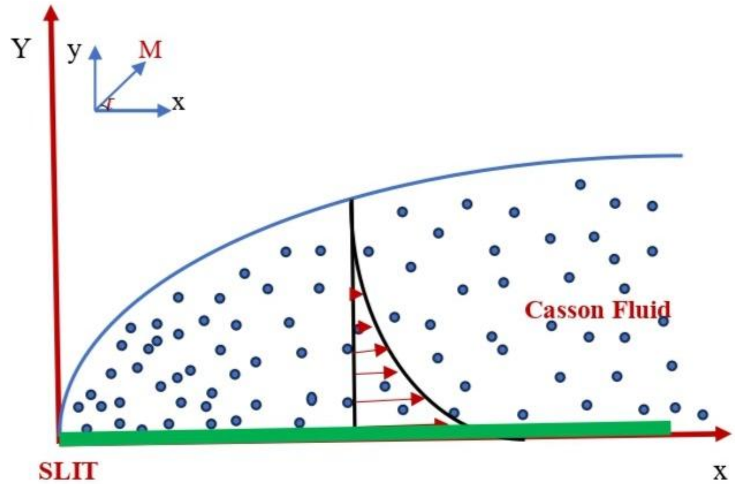


**Figure 2:** Casson fluid flow over a stretching sheet

The Governing equations for the non-Newtonian fluid flowing over a stretching sheet are given by [11, 23]:

$$\frac{\partial u}{\partial x} + \frac{\partial v}{\partial y} = 0, \tag{11}$$

$$u\frac{\partial u}{\partial x} + v\frac{\partial u}{\partial y} = \nu(1+\tfrac{1}{\beta})\frac{\partial^2 u}{\partial y^2} - (\tfrac{\sigma B_0^2 sin^2(\tau)}{\rho} + \tfrac{\mu}{\rho K})u \tag{12}$$

The corresponding boundary conditions are:

$$u = U_w, \quad v = 0 \quad at \quad y = 0 \tag{13}$$

$$u \to 0 \quad as \quad y \to \infty \tag{14}$$

The following similarities are used to convert PDE to ODE

$$u = sxf'(\eta), \quad v = -\sqrt{s\nu}f(\eta), \quad \text{and} \quad \eta = \sqrt{\frac{s}{\nu}}y. \tag{15}$$

Utilizing Eq.(26) in Eq.(23) to Eq.(25) we get

$$(1+\tfrac{1}{\beta})f''' + ff'' - f'^2 - (Msin^2(\tau) + Da^{-1})f' = 0, \tag{16}$$

corresponding boundary conditions reduce to

$$f(0) = 0, \quad f'(0) = 1 \quad \text{and} \quad f'(\infty) \to 0 \tag{17}$$

The analytic solution to this equation is

$$f(x) = \frac{1-e^{-\alpha x}}{\alpha}, \quad where \quad \alpha = \sqrt{\frac{\beta(1+Msin^2(\tau)+Da^{-1})}{1+\beta}} \tag{18}$$

**Numerical Implementation:**

To implement the present method, we need to transform a semi-infinite interval into a finite one by considering the transformation [4] $\delta = \frac{\eta}{\eta_\infty}$ and $F(\delta) = \frac{f(\eta)}{\eta_\infty}$, where $\eta_\infty$ is the number at which $f'(\eta)$ approaches zero, thus the governing equations reduce to.

$$(1+\tfrac{1}{\beta})F''' + \eta_\infty^2(FF'' - F'^2 - (Msin^2(\tau) + Da^{-1})F') = 0, \tag{19}$$

with boundary constraints:

https://doi.org/10.71058/jodac.v9i12005

$$F(0) = 0, \quad F'(0) = 1 \quad \text{and} \quad F'(1) = 0 \tag{20}$$

Now Assume

$$F'''(\delta) = D_1^T B_{y10(x)} \tag{21}$$

where $D_1^T = [\ d_1,\ d_2,\ d_3,\ d_4,\ d_5,\ d_6,\ d_7,\ d_8,\ d_9,\ d_{10}\ ]$ is an unknown coefficient matrix

On integarting Eq.(32) wrt $\delta$ from 0 to $\delta$ we get

$$F''(\delta) = F''(0) + D_1^T (S_{10\times10} B_{y10}(x) + \hat{B}_{y10}(x)) \tag{22}$$

Again integrating Eq.(33)wrt $\delta$ from 0 to $\delta$ we get

$$F'(\delta) = 1 + \delta F''(0) + D_1^T ({S'}_{10\times10} B_{y10}(x) + {\hat{B}_{y10}}'(x)) \tag{23}$$

Again integrating Eq.(34)wrt $\delta$ from 0 to $\delta$ we get

$$F(\delta) = \delta + \frac{\delta^2}{2} F''(0) + D_1^T ({S''}_{10\times10} B_{y10}(x) + {\hat{B}_{y10}}''(x)) \tag{24}$$

Now at $\delta$=1 Eq.(34) provides $F''(0)$

$$F''(0) = -1 - D_1^T ({S'}_{10\times10} B_{y10}(x) + {\hat{B}_{y10}}'(x)) \tag{25}$$

Now substituting these Eq.(24) to Eq.(28) in Eq.(22) and collocating this equation with collocating points $x_i = \frac{2i-1}{20} \quad for \quad i = 1,2,3,4,5,6,7,8,9,10$, we obtain a system of nonlinear simultaneous equations with unknown coefficients. On solving these unknown coefficients by MATLAB, we get the unknown coefficients, which on substituting in Eq.(24) to Eq.(28) we obtain $F'(\delta), F(\delta), F'''(\delta)$ and $F''(\delta)$.

The unknown coefficients $D^T$ for $\beta = 1$, $\tau = \frac{\pi}{4}$, $M = 2$, and $Da^{-1} = 2$ is:

$$D_1^T = [\ \tfrac{3699}{293}\ \ \tfrac{2474}{279}\ \ \tfrac{2377}{1364}\ \ \tfrac{-2586}{457}\ \ \tfrac{-993}{248}\ \ \tfrac{1484}{599}\ \ \tfrac{-341}{867}\ \ \tfrac{90}{3967}\ \ \tfrac{-15}{41504}\ \ \tfrac{-2}{680751}\ ]$$

$$F'(\delta) = -0.9203587392\delta^{11} - 9.264763509\delta^{10} + 31.744408858\delta^9 - 24.6143374\delta^8 - 10.302826491\delta^7 + 14.542021836\delta^6 + 5.428957081\delta^5 - 6.162474327\delta^4 - 5.0620519541\delta^3 + 7.8392087551\delta^2 - 4.227783771\delta + 0.9999999531 \tag{26}$$

The numerical implementation is similar for orthogonal polynomials as well.

Thus, for orthogonal Bessel polynomials wrt the weight function 1 we get unknown coefficients

$$D_2^T = [\ \tfrac{54997}{411}\ \ \tfrac{-17839}{59}\ \ \tfrac{11983}{82}\ \ \tfrac{-4646}{149}\ \ \tfrac{6034}{1651}\ \ \tfrac{-985}{3788}\ \ \tfrac{90}{7663}\ \ \tfrac{-13}{37954}\ \ \tfrac{1}{158722}\ \ 0\ ]$$

On substituting in Eq.(24) to Eq.(28) we obtain $F'(\delta), F(\delta), F'''(\delta)$ and $F''(\delta)$.

$$\begin{aligned} F'(\delta) = 8.9990713711\delta^2 &- 0.012665963591\delta(429\delta^6 - 693\delta^4 + 315\delta^2 - 35) \\ &- 0.00000022016314161\delta(88179\delta^{10} - 230945\delta^8 + 218790\delta^6 - 90090\delta^4 \\ &+ 15015\delta^2 - 693) - 0.000051904811991\delta(12155\delta^8 - 25740\delta^6 + 18018\delta^4 \\ &- 4620\delta^2 + 315) - 0.087486907111\delta - 30.393146191\delta^3 + 13.538996991\delta^4 \\ &+ 7.7006944711\delta^6 + 1.7544205551\delta^8 + 0.14189897941\delta^{10} \\ &- 0.305636794\delta(63\delta^4 - 70\delta^2 + 15) + 1 \end{aligned}$$

https://doi.org/10.71058/jodac.v9i12005

For orthogonal Bessel polynomials wrt the weight function $\frac{1}{\sqrt{1-x^2}}$ we get unknown coefficients $D_3^T$ as

$$D_2^T = \begin{bmatrix} \frac{-1714}{81} & \frac{15491}{248} & \frac{-6949}{113} & \frac{7536}{307} & \frac{-1419}{292} & \frac{658}{1219} & \frac{-102}{2809} & \frac{8}{4985} & \frac{-46}{909833} & 0 \end{bmatrix}$$

On substituting in Eq.(24) to Eq.(28) we obtain $F'(\delta), F(\delta), F'''(\delta)$ and $F''(\delta)$.

$$F'(\delta) = 0.00028304658590\delta(1024\delta^{10} - 2816\delta^8 + 2816\delta^6 - 1232\delta^4 + 220\delta^2 - 11) - 2.4864123880\delta(4\delta^2 - 3) - 13.30696450\delta + 0.1550274775\delta(64\delta^6 - 112\delta^4 + 56\delta^2 - 7) + 0.5146985872\delta(16\delta^4 - 20\delta^2 + 5) + 0.01098738401\delta(256\delta^8 - 576\delta^6 + 432\delta^4 - 120\delta^2 + 9) + 9.147895658\delta^2 + 11.589096980\delta^4 - 2.405654749\delta^6 - 3.080247675\delta^8 - 1.138708981\delta^{10} + 1.000000329 \quad (27)$$

**Table 5: Comparison of $f'(\eta)$ with an analytic solution for problem 3**

| $\eta$ | exact solution | Bessel Polynomial | weight function = 1 | weight fuction = $\frac{1}{\sqrt{1-x^2}}$ |
|---|---|---|---|---|
| 0 | 1 | 1.00654312625 | 1.00016565227 | 1.00000515412 |
| 1 | 0.2431167344 | 0.26451798357 | 0.24595655543 | 0.24315155627 |
| 2 | 0.0591057465 | 0.06450948283 | 0.06165465656 | 0.06016216266 |
| 3 | 0.0143695961 | 0.02653640012 | 0.01626526554 | 0.01451652626 |
| 4 | 0.0034934892 | 0.01555024073 | 0.00516556563 | 0.00356265455 |
| 5 | 0.0008493257 | 0.00245478134 | 0.00132626262 | 0.00092151558 |

**Table 6: Comparison of $(1+\frac{1}{\beta})f''(0)$ by the present method employing the Orthogonal Bessel Polynomial wrt the weight function $\frac{1}{\sqrt{1-x^2}}$ with Nadeem *et.al* [22]**

| $M$ | $\beta$ | $(1+\frac{1}{\beta})f''(0)$ by Nadeem *et.al* | $(1+\frac{1}{\beta})f''(0)$ by Present Method |
|---|---|---|---|
| 0 | 1 | 1.4142 | 1.41464251859 |
| 0 | 5 | 1.0954 | 1.095716841658 |
| 10 | ∞ | 3.3165 | 3.316825446452 |
| 10 | 1 | 4.6904 | 4.690991568547 |

https://doi.org/10.71058/jodac.v9i12005

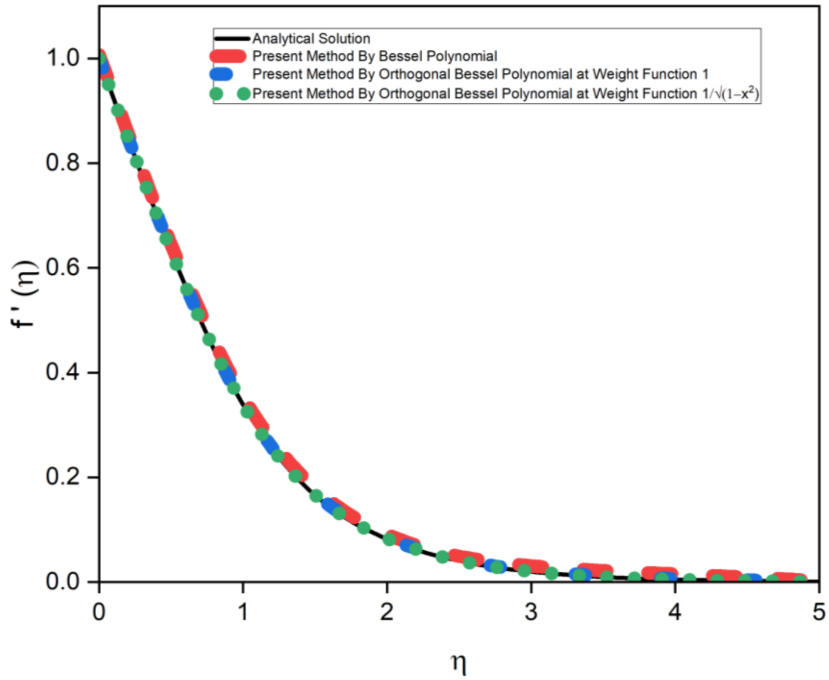


**Figure 3:** Exact versus Present method for Problem 3

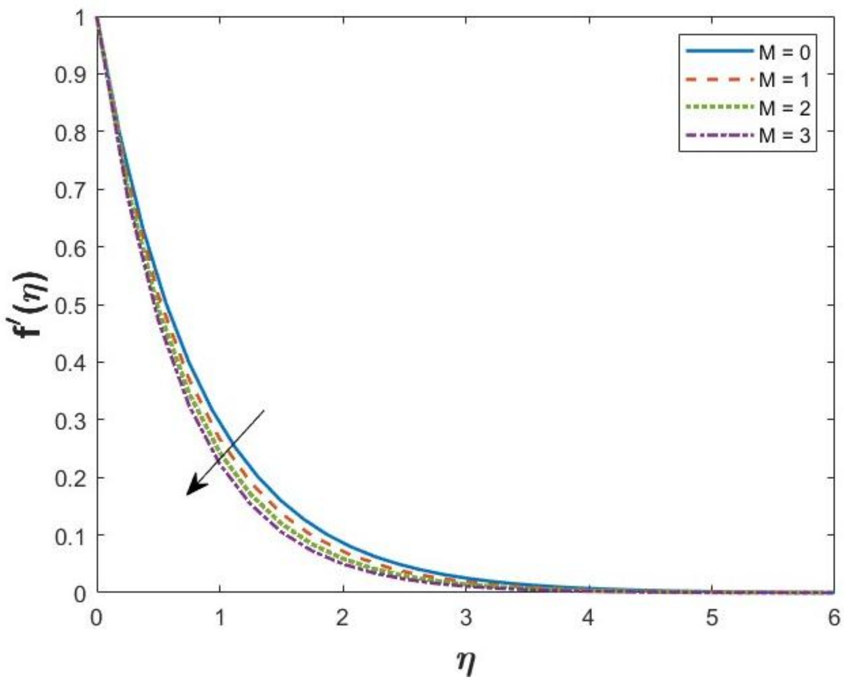


**Figure 4:** Variation of axial velocity for various values of Magnetic Field

https://doi.org/10.71058/jodac.v9i12005

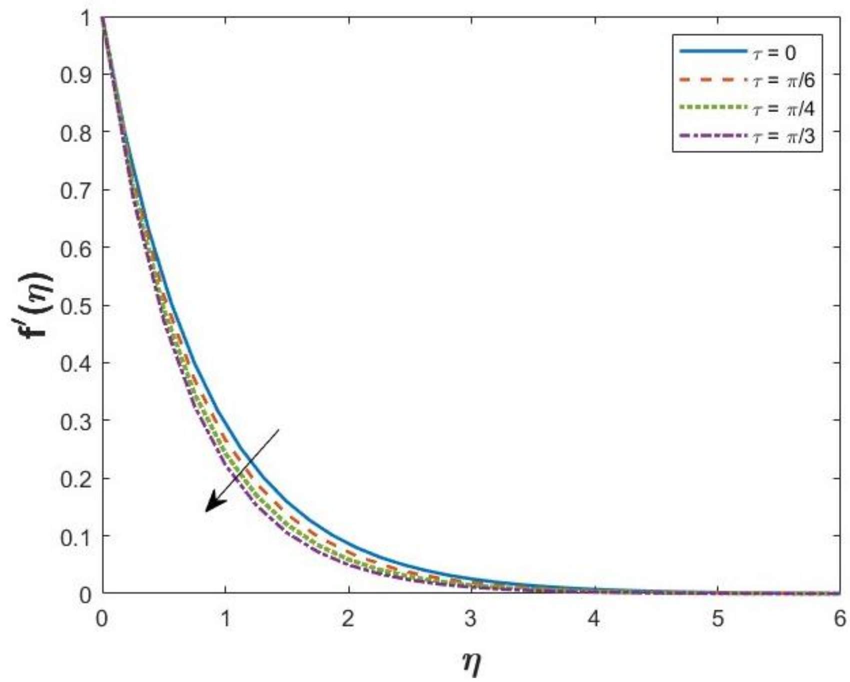


**Figure 5:** Variation of axial velocity for various values of Inclined Magnetic Field

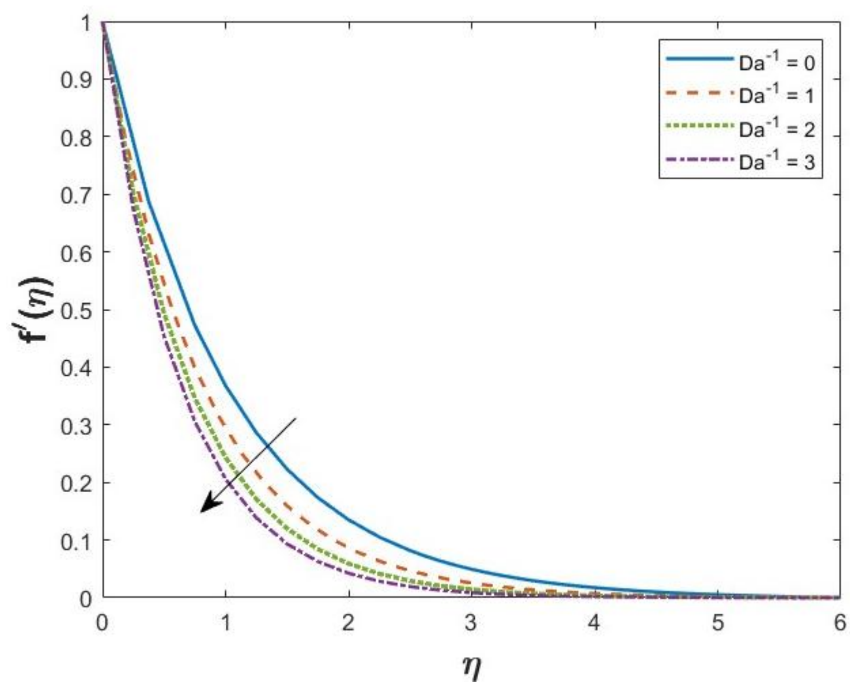


**Figure 6:** Variation of axial velocity for various values of Inverse Darcy Number

https://doi.org/10.71058/jodac.v9i12005

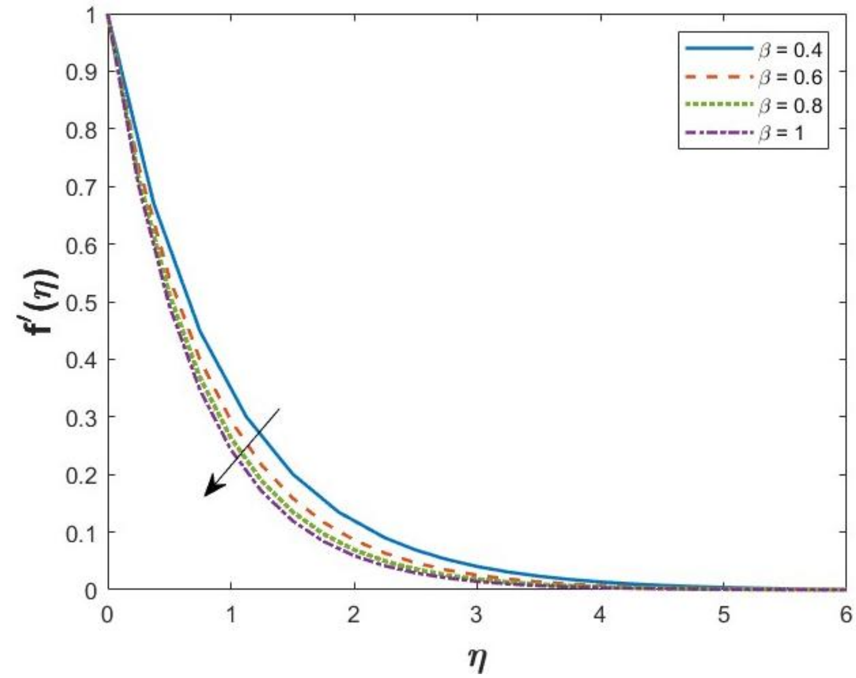


**Figure 7:** Variation of axial velocity for various values of Casson Parameter

# 5. Results and Discussions

Here a newly generated Orthogonal Bessel polynomials have been used to solve differential equations with finite and infinite boundary conditions. In problem 1, a second-order non-linear differential equation with finite boundary conditions is considered; this equation has an exact solution $cosh(x)$. The proposed method has been implemented in solving the differential equation and compared with the exact solution in Tables 2, 3 and 4. From tables, it could be observed that the absolute error is very less for orthogonal Bessel polynomials with weight function $\frac{1}{\sqrt{1-x^2}}$. Figure 1 displays the convergence of the solution via the present method with the exact solution.

In problem 2, we have considered a Casson fluid flowing over a permeable stretching sheet in the vicinity of a magnetic field that is inclined at an angle $\tau$. This problem consists of a differential equation with infinite boundary conditions. The infinite boundary condition is converted to finite by employing certain transformations and then implementing the proposed method. The solution obtained via this method has been compared with the analytical solution of the problem and found that the solution obtained is more accurate for orthogonal Bessel polynomials with weight function $\frac{1}{\sqrt{1-x^2}}$ in comparison with other polynomials, which can be witnessed in Table 5. Figure 3 displays the convergence of the solution via the present method with the analytical solution.

The graphs to study the behaviour of the fluid over the stretching sheet have been studied by employing orthogonal Bessel polynomials with weight function $\frac{1}{\sqrt{1-x^2}}$. Figure 4 shows the impact of the magnetic field on the flow. An increase in the strength of the magnetic field decreases

https://doi.org/10.71058/jodac.v9i12005

the axial velocity of the fluid due to the increased Lorentz force. Figure 5 shows the impact of an inclined magnetic field over the stretching sheet, increasing which decreases the axial velocity of the fluid. Permeability reduces the axial velocity of the fluid as shown in Figure 6, due to the increase in resistance caused by the sheet. Figure 7 displays the impact of the Casson parameter over the stretching sheet, an increase in which causes the axial velocity of the fluid to decrease.

## 6. Conclusion

In this study, we have introduced a new set of orthogonalized Bessel polynomials and deriving the operational matrix of integration corresponding to these polynomials. The generated matrices were then employed in solving a range of problems that involve both finite and infinite boundary conditions, which are commonly encountered in various engineering and physical phenomena. To assess the performance and accuracy of the method, we compared the results obtained through this approach with exact and analytical solutions available for these problems. The comparison revealed an excellent match for orthogonal Bessel polynomials with weight function $\frac{1}{\sqrt{1-x^2}}$, showcasing the precision of the developed method in solving complex differential equations. Furthermore, to provide a more visual verification of the method's effectiveness, we plotted the solutions obtained through this operational matrix approach alongside the exact solutions. The graphical comparison demonstrated a remarkable correlation between the two sets of solutions, reinforcing the high degree of precision and dependability of the suggested approach. This confirms that the orthogonalized Bessel polynomials with weight function $\frac{1}{\sqrt{1-x^2}}$, combined with the operational matrix of integration, offer a highly efficient and precise tool for solving differential equations with varying boundary conditions.

**Acknowledgement:** "I gratefully acknowledge the research fellowship received from the Karnataka DST under Award Letter No. DST/KSTePS/Ph.D.FELLOWSHIP/MP-06/2024-25, dated February 11, 2025."

## References

[1] Solsvik, J., Tangen, S., and Jakobsen, H. A. (2013). Evaluation of weighted residual methods for the solution of the pellet equations: The orthogonal collocation, Galerkin, tau and least-squares methods. Computers and Chemical Engineering, 58, 223–259. https://doi.org/10.1016/j.compchemeng.2013.07.002

[2] AlQudah, M. A. (2015). Generalized Chebyshev polynomials of the second kind. TURKISH JOURNAL OF MATHEMATICS, 39, 842–850. https://doi.org/10.3906/mat-1501-44

[3] Mccarthy, P., Sayre, J., and Shawyer, B. (1993). Generalized legendre polynomials. Journal of Mathematical Analysis and Applications, 177(2), 530–537. https://doi.org/10.1006/jmaa.1993.1275

https://doi.org/10.71058/jodac.v9i12005


[4] Shiralashetti, S. C., and Kumbinarasaiah, S. (2019). New generalized operational matrix of integration to solve nonlinear singular boundary value problems using Hermite wavelets. Arab Journal of Basic and Applied Sciences, 26(1), 385–396. https://doi.org/10.1080/25765299.2019.1646090

[5] Srivastava, H. M. (2023). An introductory overview of Bessel polynomials, the generalized Bessel polynomials and the Q-Bessel polynomials. Symmetry, 15(4), 822. https://doi.org/10.3390/sym15040822

[6] Frazier, M., and Zhang, S. (2001). Bessel Wavelets and the Galerkin analysis of the Bessel operator. Journal of Mathematical Analysis and Applications, 261(2), 665–691. https://doi.org/10.1006/jmaa.2001.7567

[7] Kumbinarasaiah, S., and Preetham, M. P. (2022). Applications of the Bernoulli wavelet collocation method in the analysis of MHD boundary layer flow of a viscous fluid. Journal of Umm Al-Qura University for Applied Sciences, 9(1), 1–14. https://doi.org/10.1007/s43994-022-00013-6

[8] R, V. S., S, P., and B, P. M. (2024). Application of the Fibonacci wavelet approach to the MHD boundary layer analysis of a Casson fluid past a stretching sheet. Numerical Heat Transfer Part B Fundamentals, 1–22. https://doi.org/10.1080/10407790.2024.2350684

[9] Shree, R. V., Mallikarjun, B. P., and Chamkha, A. J. (2024). Analysis of MHD boundary layer flow of a viscous fluid past a stretching sheet employing the Legendre wavelet method. International Journal of Ambient Energy, 45(1). https://doi.org/10.1080/01430750.2024.231062

[10] Shree, R. V., Mallikarjun, B. P., and Kumbinarasaiah, S. (2024b). Time-varying stretching velocity analysis for an unsteady flow of Williamson fluid by Hermite wavelet. Journal of Umm Al-Qura University for Applied Sciences, 10(3), 541–554. https://doi.org/10.1007/s43994-024-00126-0

[11] Prithvi, S., Shree, R. V., and Mallikarjun, B. P. (2025). Analyzing MHD Williamson Fluid Over A Porous Stretching Sheet with Heat and Mass Transfer by Applying the Chebyshev Wavelet Operational Matrix Method. International Journal of Applied and Computational Mathematics, 11(2). https://doi.org/10.1007/s40819-025-01838-5

[12] Ramareddy, V., Basawaraj, P. M., Mahabaleshwar, U. S., and Souayeh, B. (2024). An MHD boundary layer flow of Casson fluid due to a moving wedge analyzed by the Bernoulli wavelet method. ZAMM - Journal of Applied Mathematics and Mechanics / Zeitschrift Für Angewandte Mathematik Und Mechanik, 104(4). https://doi.org/10.1002/zamm.202300648

[13] Shiralashetti, S. C., Joshi, S. S., and Hanaji, S. I. (2025). Bernoulli wavelet analysis of mixed convective magnetohydrodynamic boundary layer flow of Casson nanofluid over inclined stretching sheet with entropy generation. Multiscale and Multidisciplinary Modeling Experiments and Design, 8(3). https://doi.org/10.1007/s41939-025-00772-9

[14] Yadav, N. K., and Sinha, R. K. (2025). Bernstein wavelets based numerical algorithm for solving fractional order lumpy skin disease model. Journal of Nonlinear Complex and Data

Science. https://doi.org/10.1515/jncds-2024-0090

[15] Soleyman, F., and Area, I. (2025). Müntz–Legendre Wavelet Collocation Method for solving fractional Riccati equation. Axioms, 14(3), 185. https://doi.org/10.3390/axioms14030185

[16] Suresh, P., Ramareddy, V. S., and Basavaraj, P. M. (2025). Analyzing MHD boundary layer flow of Rivlin Ericksen fluid over a stretching sheet by applying Taylor Wavelet Approach. Computational Methods for Differential Equations.

[17] Shiralashetti, S. C., Pala, V. R., and Hanaji, S. I. (2025). Jacobi wavelet integration operational matrix method for the numerical solution of laminar nanofluid flow problem. International Journal of Ambient Energy, 46(1). https://doi.org/10.1080/01430750.2025.2458178

[18] Mulimani, M., and Kumbinarasaiah, S. (2024). Gegenbauer wavelets collocation technique for the nonlinear Fisher's reaction–diffusion equation with application arising in biological and chemical sciences. International Journal of Dynamics and Control, 13(1). https://doi.org/10.1007/s40435-024-01508-2

[19] R, V. S., B, P. M., Souayeh, B., and Bhattacharya, S. (2024). Application of Fibonacci wavelet frame operational matrix for the analysis of Arrhenius-controlled heat transfer flow in a microchannel. Case Studies in Thermal Engineering, 105326. https://doi.org/10.1016/j.csite.2024.105326

[20] Dong, Y., and Chen, G. (2025). An effective numerical algorithm for a system of fractional pantograph delay differential equations based on the Haar wavelet collocation method. The Journal of Supercomputing, 81(4). https://doi.org/10.1007/s11227-025-07028-w

[21] Raza, A., Alam, M. P., and Faheem, M. (2025). An effective Hermite wavelet collocation method for 3D partial differential equations with convergence analysis. Journal of Applied Mathematics and Computing. https://doi.org/10.1007/s12190-025-02422-2

[22] Nadeem, S., Haq, R. U., Akbar, N. S., and Khan, Z. (2013). MHD three-dimensional Casson fluid flow past a porous linearly stretching sheet. Alexandria Engineering Journal, 52(4), 577–582. https://doi.org/10.1016/j.aej.2013.08.005

[23] Ahmad, K., Wahid, Z., and Hanouf, Z. (2019). Heat transfer analysis for Casson fluid flow over stretching sheet with Newtonian heating and viscous dissipation. Journal of Physics Conference Series, 1127, 012028. https://doi.org/10.1088/1742-6596/1127/1/012028

[24] Prithvi, S., Mallikarjun, B. P., Bhattacharyya, S., & Biswas, N. (2025). Newly generated path graph matching-polynomial matrix of integration to solve initial-value, finite-value and infinite-boundary-value problems. *The European Physical Journal Special Topics*. https://doi.org/10.1140/epjs/s11734-025-01933-0